International Journal of Geology and Earth Sciences

ISSN 2395-647X www.ijges.com
Vol. 5, No. 2, June 2019
doi:10.32937/IJGES.5.2.2019.73-95

Research Paper

Geomechanical Property Evolution and the Mechanics of Growth Faulting in a Niger Delta oilfield, Nigeria

Fidelis A. Abija[1,2]

Corresponding Author: **Fidelis A. Abija ✉ fidelabija@yahoo.co.uk*

Received on: 18th April, 2019 Accepted on: 22nd May, 2019

Subsurface rocks' response to stress and the attendant deformation is a function of the geomechanical properties under in situ pore pressure conditions. Understanding rock behavior in vertical and lateral successions, the effects of stress on the rock sequences which often cause compartmentalization and defining fluid communication within the basin is necessary for optimizing drilling, completion and production. Rock cores are seldom available for laboratory test hence use of dynamic method. The mechanical properties and local deformation in a depth interval of 1500m and 4500m have been using wireline logs. Results shows that the mechanical property evolution was influenced by rock mineralogy, porosity, depth of burial, pore pressure, effective stress, tectonics and temperature. Increase depth of burial and effective vertical stress favoured syndepositional compaction and paleotectonic stresses greater the rock strength induced tensile fracturing and faulting culminating in kinematic translation and creation of a depositional centre in the middle of the field. Rapid progradation of sandstones and shales sequences due to marine incursion created both stratigraphic and structural compartmentalization. This accompanied by low rate of fluids diffusion and imposition of overburden load on the pore fluids, vertical transfer along the faults, grain sliding in shear; reduction in the rock compressibility and pore volume; and destruction of cement bonding causing compaction disequilibrium and generating excess pore pressure in the shales. Re - orientation of the tectonic stresses led to elastic stretching of the ductile and high elasticity shales and microfracturing of the brittle sandstones forming growth faults and rollover anticlines that favoured hydrocarbon migration from the lower Akata source rock into the porous reservoirs and shale capping and smearing on the fault limbs providing the trapping mechanism..

Keywords: Petrophysical logs, mechanical properties, rock deformation, growth fault, roll over anticlines

[1] Centre for Geomechanics, Energy and Environmental Sustainability, Port Harcourt, Nigeria.
[2] B. J. Anderson Engineering Ltd, Km 20, Airport Road, Port Harcourt, Nigeria.

Introduction

Stresses in the earth cause rock deformations resulting to change of shape, size and or volume whether in a simple subsiding basin or at colliding plate boundaries (Cook et al 2007). A rock's response to stress depends on its composition which gives it characteristic mechanical properties. Understanding present day crustal stresses is critical to interpretations of continental scale plate tectonic induced deformations and geomechanics is concerned with the mechanical response of all geological materials to these force fields and their hazards (Turner et al 2017). The mechanical properties of a rock in the earth are those characteristics which determine its behavior under different conditions of stress and are classified into elastic and anelastic based on their elasticity. Rock deformation which is either elastic or plastic may be caused by tension, compression or shear and this can result in compaction, extension, translation or rotation eventually ending in shearing, fracturing or faulting. Elastic deformation can be restored when the rock is relived of the applied stress while plastic deformation is permanent when the critical threshold value of the rock strength is exceeded in the ductile field thus leaving permanent alteration in the rock's volume, shape and fluid flow path (Fjaer et al 2008).

Rock response to stress depend on composition, cementation, porosity and burial depth and could result in alteration of rock volume, geometry, permeability, porosity, rock strength, elasticity and paths of fluid flow. Rocks rupture under brittle deformation and most rock mechanics applications are based on linear elasticity. However, most sedimentary rocks exhibit plastic behavior and creep (Fjaer et al 2008).

The mode of geological force and type of geological media to a large extent determine the effects of the force and the behavior of the rock. Consequently, four types of rock behavior and corresponding deformations may occur as well as three elastic moduli that correspond to each type of deformation. Geomechanical properties of rock formations evolve over time during the process of deposition and sedimentation under the influence of gravitational and tectonic stresses, fluid pressure, thermal stress, and post depositional diagenetic reactions within the cement bonds. These processes are important in oil/gas field evolution, hydrocarbon source migration and accumulation as they determine rock structures such as folding, fracturing, faulting, diapirism, and post depositional compaction.

Geomechanics has found wide application in Petroleum exploration and production including but not limited to pressure prediction, wellbore stability, sand control and management, reservoir production management, geosteering, horizontal well design (Abija and Tse 2016), fracture permeability, stage placement of hydraulic fracture, multilateral wells and multiple well completions, drill cutting re-injection and effluent subsurface storage design, geosequestration and carbon emissions control, reservoir compaction and subsidence prediction (Pietro et al 2010), modeling fault zone hydrogeomechanical coupling and hydrocarbon migration into groundwater aquifers. Extending the life of oil and gas field and deriving optimal benefit from the investment is assured through proactive geomechanical field evaluation and design (Zoback et al 2003).The complexity and cost of oil/gas well planning and development in terms of geometry (reach and length) and access to deep, high-temperature,

over pressured and high-stress regimes requires integrating geology and the mechanics of tectonic processes for a more economic field planning and design. Characterization of the geomechanical responses of rocks to stress is based on critical understanding of the processes that act within the earth, their interactions and effects on in situ rocks throughout the geologic evolution of the basin and this is required for field planning and development. Rock compressibility for example is essential for compaction and subsidence evaluation, reservoir drive determination, reserve estimation, reservoir pressure maintenance, casing collapse analysis and production forecasting (Geerstma 1973, Wolf et al 2005), Bruno 2001), Poisson ratio is an input parameter in hydraulic fracture design (Schlumberger 1989, Anderson 2006, Cleary 1958), stress path and reservoir depletion analysis, rock strength for sand prediction and wellbore strengthening analysis (Schlumberger 1989) etc.. Induced stress changes caused by drilling, injection, fracturing and production causes re-orientation of the principal stresses thus affecting the rock properties, wellbore stresses and rock responses capable of causing shear, tensile and compressive failures. This research was carried out to evaluate the geomechanical properties in the oilfield, their responses to stress gravitational and tectonic stresses during the basin evolution through to the present day and their impacts on the petroleum system.

Study Area

Location and Geologic Setting

The study area is located in the onshore coastal swamp within 05 13.2208°N and 006 41.0107°E situated in the Gulf of Guinea (Figure 1). The basin, one of the largest regressive deltas, is estimated to cover an area of 300,000 km^2 with a sediment volume of 500,000 km^3 (Hospers 1965), and a sediment thickness of over 10 km in the depocenter (Kaplan et al 1994). A southwestward progradation during basin evolution formed depobelts that represent the most active portions of the delta at each stage of its evolution (Doust and Omatsola 1990, Kulke 1995). Estimates of recoverable hydrocarbons are about 34.5 billion barrels of oil and 93.8 trillion cubic feet of gas (14.9 billion barrels of oil equivalent) per unit volume of basin-fill. The stratigraphic sequences of the basin are subdivided into three units namely Akata, Agbada and Benin formations each of which range from Tertiary to Recent (Short and Stauble 1965).

The onshore portion of the Niger Delta Province is delineated by the geology of southern Nigeria and southwestern Cameroon. The Benin flank, an East-North East trending hinge line south of the West Africa basement massif marks the boundary north-westward while Cretaceous outcrops of the Abakaliki High forms the northeastern boundary. The Calabar flank, a hinge line bordering the adjacent Precambrian, forms the East-South-East limit of the basin. Offshore, the basin is bounded by the Cameroon volcanic line to the east, the eastern boundary of the Dahomey basin (the eastern-most West African transform-fault passive margin) to the west, and the two-kilometer sediment thickness contour or the 4000m bathymetric contour in areas where sediment thickness is greater than two kilometers to the south and southwest. This forms the geologic extent of the Tertiary Niger Delta (Akata-Agbada) Petroleum System.

Geotectonic Setting

Tectonically, basin evolution was controlled by Cretaceous fracture zones formed during the

Figure 1: Map of Study Area Showing Studied Wells (Inset Map of the Niger Delta)

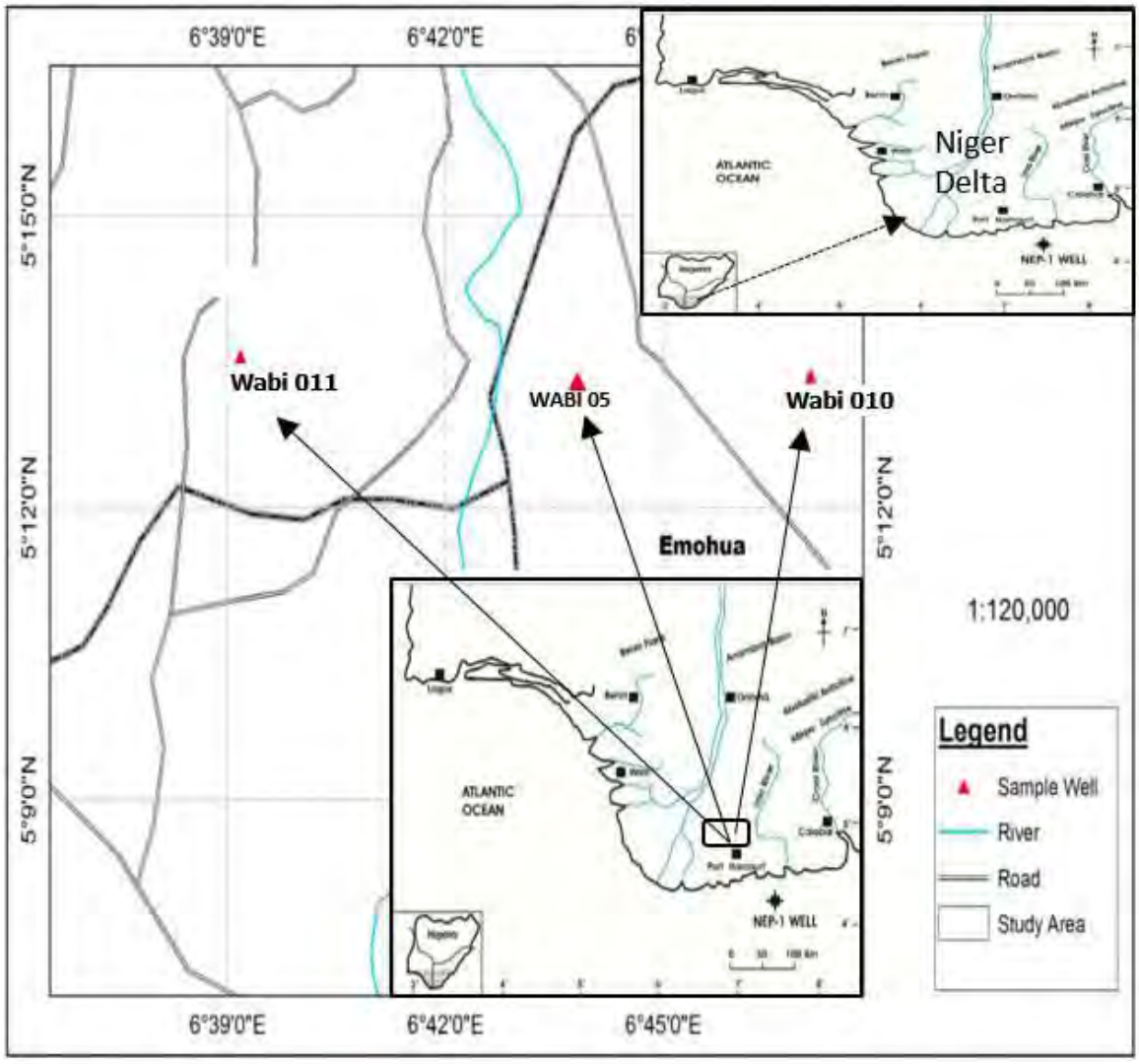

triple junction rifting and opening of the south Atlantic which palaeo-indicators include trenches and ridges in the deep Atlantic. Fracture zone ridges subdivide the margin into individual basins and forms the boundary faults of the Cretaceous Benue Abakaliki trough that cuts far into the West African shield.

The trough, an aulacogen of the triple junction rift system, started opening in the Late Jurassic and persisted into the Middle Cretaceous (Lehner and De Ruiter 1977) diminishing in the Niger Delta during the Late Cretaceous.This was followed by gravity tectonism as the primary deformational process after cessation of rifting and induced deformation in response to shale mobility (Kulke 1995). Shale diapirism due to loading of poorly compacted, over-pressured, prodeltaic and delta-slope clays resulted in the deposition of the Akata

Formation, the continental intercalaire by the higher density delta-front sands of the Agbada Formation. This was followed by slope instability caused by lack of lateral basinward support for the under-compacted delta slope clays of the Akata Formation. Gravity tectonics indexed by structures such as shale diapirs, roll-over anticlines, collapsed growth fault crests, back-to-back features, and steeply dipping closely spaced flank faults (Evamy et al 1978) completed the pro-deltaic deposition before deposition of the Benin Formation. These faults mostly offset different parts of the Agbada Formation and flatten into detachment planes near the top of the Akata Formation. Deposition of the formations in offlapping siliciclastic sedimentation cycles 30-60Km wide, prograde southwestward 250Km over oceanic crust into the Gulf of Guinea (Stacher 1995) and synsedimentary faulting occurred in response to variable rates of subsidence and sediment supply (Weber and Daokoru 1977). Subsidence and supply rates interplay resulted in deposition of discrete depobelts. When further crustal subsidence could no longer be accommodated, the centre of sediment deposition shifted seaward forming new depobelt each marking a break in regional dip of the delta bounded landward by growth faults and seaward by large counter regional faults or the growth fault of the next seaward belt (Evamy et al 1978**)**. Each depobelt is a separate unit recognized by its own sedimentation, deformation, and petroleum history. Doust and Omatsola (1990) describe three depobelt provinces based on structure. The northern delta province which overlies relatively shallow basement has the oldest growth faults that are generally rotational, evenly spaced with increase steepness seaward. The central delta province has depobelts with well-defined structures such as successively deeper rollover crests that shift seaward for any given growth fault. The distal delta province is the most structurally complex due to internal gravity tectonics on the modern continental slope.

Study Materials and Methodology

The materials used include wireline log data namely density, sonic, resistivity and gamma ray provided by Total E&P Nig. Ltd, through the Department of Petroleum Resources, (DPR), Port Harcourt, Nigeria. The dynamic method of property determination was employed. Geotechnical properties of rocks are traditionally determined from laboratory testing of cored samples. However, in oil and gas wells, these are seldom available for pre-drilling testing and design. petrophysical logs usually available in all offset wells are utilized for the determination of rock properties empirical equations that utilize rock density, sonic compressional ($ÄT_C$) and shear ($ÄT_S$) slownesses. The derived empirical equations applied in this research are based on the fact that, the factors which affect the formation parameters such as velocity, porosity and elastic moduli equally affect rock strength and other geomechanical properties (Sinha et al 2008). The theory of derivation is based on the principles of acoustoelasticity effects in which changes in rock elastic wave velocities are caused by changes in pre-stress in the propagating medium. These empirical relations employ one or more of P - wave velocity or interval transit time which is directly measured in sonic logging, elastic modulus derived from velocity of P - wave and density - porosity usually derived from density measurements using rock matrix and fluid

densities (Sinha et al 2008, Chang et al 2006). It is noteworthy that dynamic properties require calibration to static in situ conditions using core geomechanical laboratory test results. In this study, cores were not available for this tests thus a limitation in calibration of the model results. In the field of study, shear slowness data were not available in well 05 necessitating the calculation of P-wave velocity from the compressive slowness and results used to derive the shear wave velocity. This was achieved using the relationships in the equations (1), (2), (3) and (4) (Crain and Holgate 2004, Greenberg and Castagna 1993).

$$V_n = \frac{10^6}{\Delta T_c} \quad ...(1)$$

$$V_s = \frac{10^6}{\Delta T_s} \quad ...(2)$$

ÄT$_S$

V_s = (0.804 x V_p) – 0.856 (sand) ...(3)

V_s = (0.769 x V$_p$) – 0.0.867 (shale) ...(4)

The derived empirical relations are especially useful where cores are not available for mechanical tests and modeling are performed based on empirical correlations from measurable physical properties obtainable from wireline logs normally available for all offset wells within the field for pre-drilling analysis and design (Paul and Zoback, 2008). They can also be used in early stages of a new prospect, re-evaluating of old assets, or simply as a preliminary tool prior to designing a geomechanical test schedule (Azizi and Memarian, 2006). The results of this analysis are applicable in hydrocarbon as well as geothermal energy development.

Each of the rock mechanical properties was calculated using the equation for the parameter as defined.

Poisson Ratio (*v*)

The Poisson ratio was computed from P and S wave velocities calculated from the acoustic slownesses (ÄT$_c$) and (ÄT$_s$) using equation (5) (Jones et al 1992, Moos 2006).

$$v = 0.5(V_p/V_s)^2 - 1/(V_p/V_s)^2 - 1 \quad ...(5)$$

Shear Modulus (G)

The shear modulus is the ratio of the shear stress to the shear strain which for a homogeneous, isotropic and elastic rock it's given by equation (6) (Schlumberger 1989),.

$$G = 13464 \times \rho_b / \Delta T_S \upsilon \quad ...(6)$$

where coefficient a = 13464, ρ_b= bulk density in g/cm^3, ΔT_s = Shear sonic transit time in μS/ft. The unit of *G* is 10^6 psi which can be converted to MPa.

Bulk Modulus (K$_B$)

The bulk modulus (K_b) is a static modulus but an equivalent dynamic modulus an was computed using eqn. 7 from the sonic and density logs.

$$K_b = a\rho_b(1/\Delta T_C^2 - 4/3ÄT_S^2) \quad ...(7)$$

where coefficient a = 13464, ρ_b= bulk density in g/cm^3, ΔT = sonic transit times for compressional and shear wave in μS/ft. The unit of K$_b$ is 10^6 psi.

Matrix/Grain Bulk Modulus (K$_m$)

$$K_m = KS\ \rho_{ma}/(1/\Delta T_{Cma}^2 - 4/3\Delta T_{Sma}^2) \quad ...(8)$$

where *KS* is constant and = 1000 if ΔT is in μs/m and 13400 μs/ft,

Elastic Modulus (E)

Elastic modulus was determined from the relationship between Young's modulus, shear modulus and Poisson ratio in equation (9).

$$E = 2G\ (1 + \mu) \quad ...(9)$$

where G = shear modulus and μ = Poisson ratio. E is in psi.

Bulk Compressibility (C_b) With Porosity

$$C_b = 1/K_b \quad ...(10)$$

Rock Compressibility (C_R) ZERO POROSITY

$$C_r = 1/(a\rho_{log}(1/\Delta T_{Cma}{}^2 - 4/3\ \Delta T_{Sma}{}^2) \quad ...(11)$$

BIOT CONSTANT (α)

Biot's coefficient is a constant introduced into Terzaghi's effective stress and the uniaxial strain equation as a factor to account for resistance of the rock frame against deformation as pore pressure changes (Biot, 1941). It describes how much of the stress and pore pressure changes is converted to effective stress change. It is dependent on compressibility, bulk modulus and porosity and varies in the range of porosity and 1. When it is one, Terzaghi's original effective stress and the uniaxial strain equations are realized (Fjaer et al 2008). It was determined using the expressions in equations (12) and (13).

It is expressed as

$$\alpha = 1 - K_b/K_m \quad ...(12)$$

in terms of bulk and grain modulus where K_b and k_m are skeleton bulk and solid grain moduli respectively [28]. In terms of compressibility, it is expressed as

$$\alpha = 1 - C_f/C_b \quad ...(13)$$

where C_r and C_b are grain and bulk compressibility respectively.

Uniaxial Compressive Strength (UCS)

Equation (14) (McNally 1987) which is applicable in fine grained consolidated and unconsolidated sandstones within all porosity ranges is suited for the Niger Delta basin and was applied.

$$UCS = 1200\ exp^{(-0.036\Delta Tc)} \quad ...(14)$$

Lal (1999) proposed equation (15) for shales based on rock cores from the North Sea basin

$$UCS = 10(304.8/\Delta T_c - 1) \quad ...(15)$$

where UCS = unconfined compressive strength in psi, ΔT_c = compressional wave transit time.

Cohesion (C_o)

The cohesive strength was determined using (Coates and Denoo 1981**)** equation (16)

$$C_o = 5(V_p - 1)/0.5(V_p) \quad ...(16)$$

Friction Angle(FA)

Lal (1999) equation (17) which uses the velocity of compressional wave, was adopted for the determination of angle of friction.

$$\phi = Sin^{-1}(V_p - 1/V_p + 1) \quad ...(17)$$

where ϕ is angle of friction, V_p is velocity of p-wave.

Tensile Strength (T_o)

Equation (18), (Coates and Denoo, 1981) was used evaluating tensile strength.

$$T_o = C_o/12 \quad ...(18)$$

Shear Strength

The initial shear strength was determined using the empirical relation (19) by (Schlumberger 1989).

$$\tau_i = 0.026E/C_b \times 10^6\{0.008V_{sh} + 0.0045(1 - V_{sh}) \quad ...(19)$$

where E = Elastic modulus in psi, C_b = bulk compressibility in psi^{-1} and V_{sh} = volume of shale in fraction,

Determination of Petrophysical Parameters

Volume of Shale

The shale volume is the bulk volume of the reservoir composed of clay minerals and clay bound water. It was determined using equation (20) (Larinov 1962).

$$V_{shale} = 0.083(2^{3.7Igr} - 1) \quad ...(20)$$

where I_{gr} is the shale index (gamma ray index) which is defined in (21)

$$I_{gr} = \frac{GR_{log} - GR_{min}}{GR_{max} - GR_{min}} \quad ...(21)$$

where, GR_{log} = measured gamma ray log reading at depth *z,* GR_{min} = minimum gamma ray log in clean sand, GR_{max} = maximum gamma log reading (in clean shale), V_{shale} = volume of shale in the formation at depth *z*.

Porosity

Porosity is the total volume of a rock occupied by pores both connected and unconnected. It is the ration of the pore volume to the bulk volume expressed as fraction or %. Porosity is determined from density, sonic, neutron logs.

The total porosity was determined from density log data which are weighted average densities of the rock and pore fluid using equation (22).

$$\Phi_D = (\rho_{ma} - \rho_b)/(\rho_{ma} - \rho_{fl}) \quad ...(22)$$

where Φ_D = total density porosity, ρ_{ma} = density of rock matrix, ρ_b = measure density and ñ$_{fl}$ = density of fluid. Shale corrected density was calculated by application of volume of shale using equation (23).

$$\Phi_{eff} = (\rho_{ma} - \rho_b)/(\rho_{ma} - \rho_{fl}) - V_{sh}(\rho_{ma} - \rho_{sh})/(\rho_{ma} - \rho_{fl}) \quad ...(23)$$

where Φ_{sh} is shale corrected density porosity, V_{sh} is volume of shale and ρ_{sh} is density of shale.

The results of this analysis were plotted in log format using Petrel 2010 and correlated across the wells.

Results and Discussion

Mechanical Property Evolution

The mechanical property evolution of the basin's field was influenced by the rocks' mineralogy, porosity, depth of burial, pore pressure, effective stress, tectonics and temperature. Increase depth of burial and effective vertical stress due to overburden loading favoured syndepositional compaction of the intervening sequences of sandstone and shales, tectonic induced tensile fracturing and faulting culminating in kinematic translation.

These processes imparted higher strength on the rocks as seen in the uniaxial compressive strength, cohesive strength, tensile strength and elastic modulus which vary from 20.21MPa, 5.8MPa, 1.68MPa, and 6.69 x 10^{-9} MPa respectively at 1500m to 32.11MPa, 6.59MPa, 2.69MPa and 1.47 x 10^{-9}MPa at 2500m in the in the shales formations of well 11, east of the field. The strength of sandstones was significantly increased from 38.7MPa, 7.14MPa, 2.89MPa and 2.34 x 10^{-8}MPa respectively at 3000m to 78.44mPa, 7.35MPa, 6.64MPa and 2.96 x 10^{-8} MPa for uniaxial compressive strength,

cohesive strength, tensile strength and elastic modulus respectively (Table 1 and 2 and fig. 2a). The trend of increasing strength with depth was also visible in well 5 which constitute the downthrown block with results ranging from 15.39MPa, 9.99MPa, and 1.28MPa at 1500m to 28.84MPa, 10.34MPa, and 2.40MPa at 2500m for uniaxial compressive strength, cohesive strength, and tensile strength in the shales but with decrease in elastic modulus from and 53,037.6MPa to 51,412.95MPa (Tables 1 and 2 and Figure 2b). This decrease in elastic modulus is consistent with increase sediment loads, rapid sedimentation rates, compaction disequilibrium and aquathermal effects. In well 10 west of the field, the strength decreased respectively as 24.95MPa, 6.45MPa, and 2.08MPa for uniaxial compressive strength, cohesive strength, tensile strength and elastic modulus in shales at 2000m to 23.99MPa, 6.78MPa and 1.99MPa for uniaxial compressive strength, cohesive strength and tensile strength of shales at 3000m depicting reduction in the bulk density of the rock minerals and reduced intensity of compaction. The elastic modulus however increased from 18,644.8MPa to 19382.5MPa. Overpressure generation in

Table 1: Rock Elastic Properties in the Field

Well	Depth(m)	Rock Type	v	K_o	GMP_a	K_bMpa	EMpa	C_bMPa^{-1}	C_rMPa^{-1}	α
Well 10	2000	Shale	0.33	0.49	7000.77	18,455.3	18,644.8	2.58×10^{-9}	5.96×10^{-4}	1
	2500	Shale	0.34	0.52	8,717.91	253,312.8	23,466.1	1.87×10^{-9}	5.96×10^{-4}	1
	3000	Shale	0.33	0.50	7,262.97	19,500	19,382.5	2.44×10^{-9}	5.96×10^{-4}	1
	3500	Sandstone	0.21	0.27	2,877.3	4,112.19	7,003.8	1.15×10^{-9}	5.96×10^{-4}	1
	4000	Sandstone	0.27	0.37	4,845.13	8,947.59	12,312.9	$5.31E \times 10^{-9}$	6.0×10^{-4}	1
Well 5	1500	Shale	0.35	0.52	69.8	188.4	53,037.6	2.52×10^{-6}	2.45×10^{-6}	0.9
	2000	Shale	0.34	0.52	69.38	186.4	51,412.9	3.54×10^{-4}	-3.1×10^{-3}	0.9
	2500	Shaly SST	0.33	0.48	68.13	180.99	54,769.9	3.33×10^{-3}	-9.65×10^{-2}	0.9
	3000	Sandstone	0.26	0.35	58.86	148.42	55,167.5	2.91×10^{-3}	-1.31×10^{-7}	0.9
	3500	Sandstone	0.22	0.29	58.99	145.1	55,413.4	2.64×10^{-3}	-1.72×10^{-7}	0.9
	4000	Sandstone	0.27	0.37	59.96	152.49	55,390.5	2.97×10^{-3}	-0.0344	0.9
Well11	1500	Shale	0.37	0.60	2.43×10^{-6}	5.5×10^{-10}	6.69×10^{-10}	86,773.1	5.96×10^{-4}	1
	2000	Shale	0.35	0.55	3.3×10^{-9}	8.8×10^{-10}	9.03×10^{-9}	545,787.1	5.96×10^{-4}	1
	2500	Shaly SST	0.32	0.47	5.6×10^{-9}	1.7×10^{-9}	1.47×10^{-8}	27,320.3	5.96×10^{-4}	1
	3000	Sandstone	0.27	0.37	$9.2E \times 10^{-9}$	4.7×10^{-9}	2.34×10^{-8}	13,380.6	5.96×10^{-4}	1
	3500	Sandstone	0.25	0.33	1.1×10^{-7}	6.2×10^{-9}	2.89×10^{-8}	9,992.7	5.96E-4	1
	4000	Sandstone	0.18	0.23	1.2×10^{-8}	6.2×10^{-9}	2.96×10^{-8}	7,749.2	5.96×10^{-4}	1

Note: v = Poisson ratio, $K_o = v/1 - \mu$, G = modulus of rigidity, K_b = bulk modulus, Young's modulus, C_b – bulk compressibility, C_r = grain compressibility, α = Biot's coefficient, SST = sandstone

Figure 2a: Well 11 Mechanical Property Log

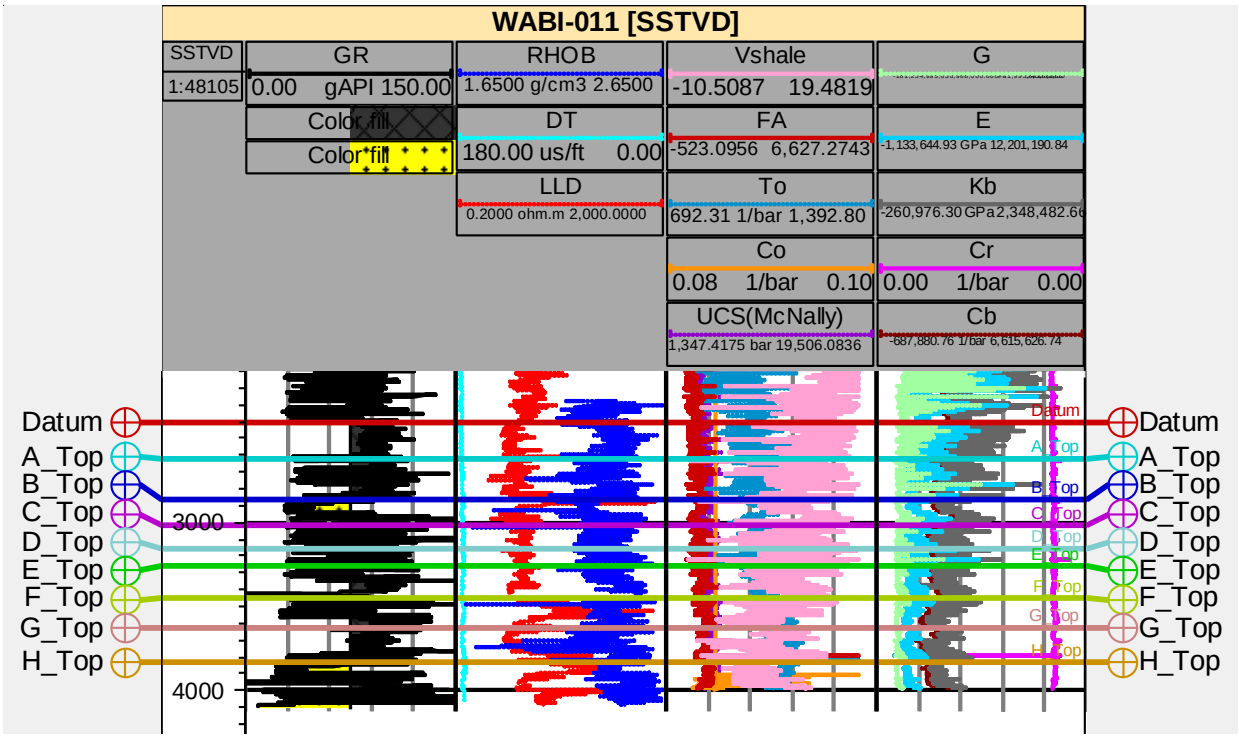

Figure 2b: Well 5 Mechanical Property Log

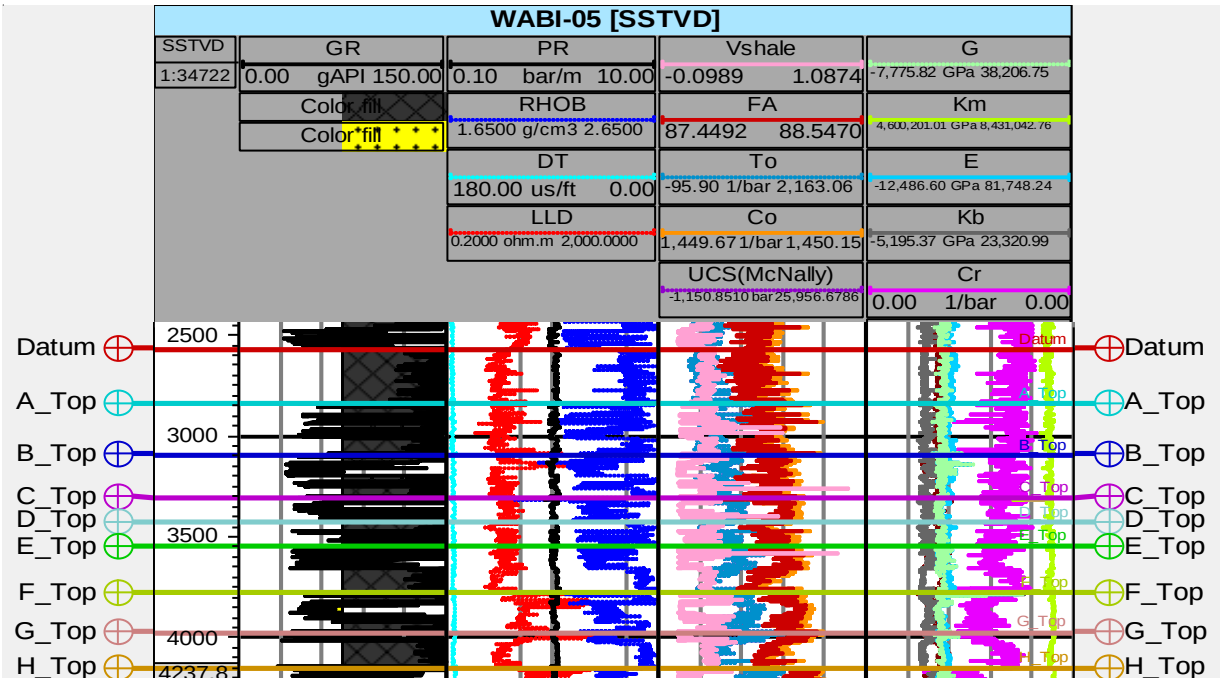

Figure 2c: Well 10 Mechanical Property Log

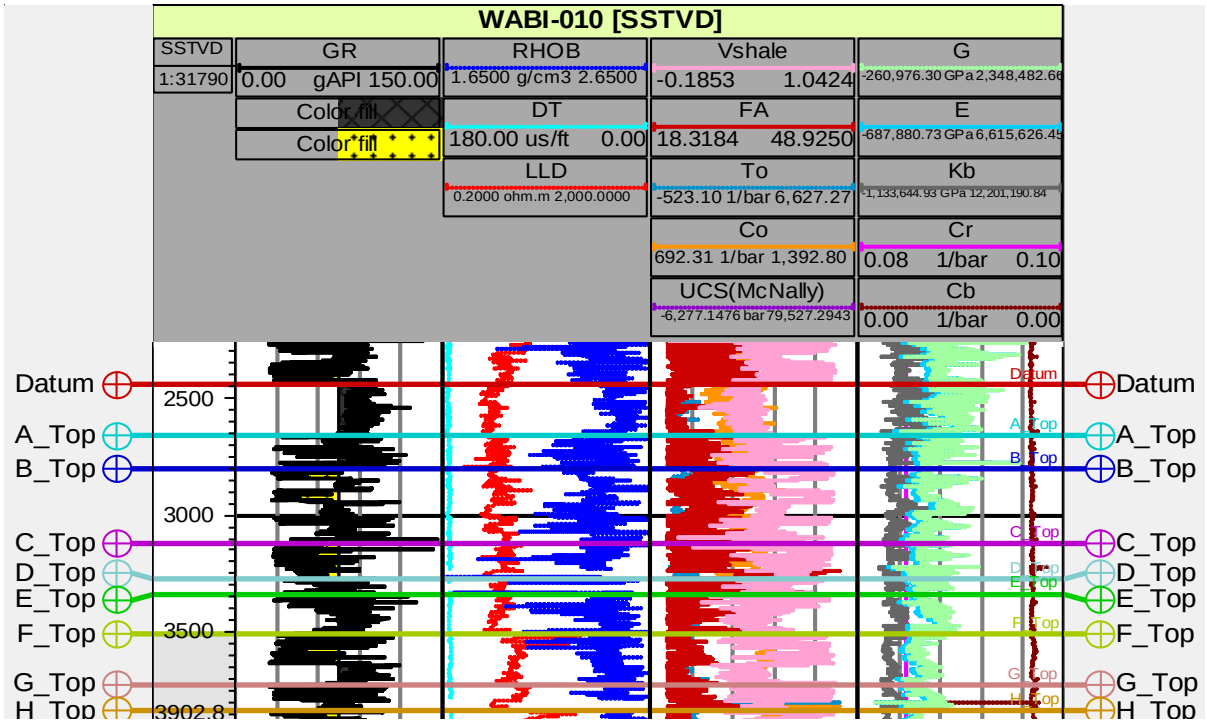

response to increase load and fluid trapping to redistribute the locked in stresses and achieve equilibrium is attributed as the causal factor for increase elasticity of the ductile shales. The uniaxial compressive and tensile strengths of the sandstones in well 10 decreased from 89.03MPa, and 7.42MPa at 3500m to 53.06MPa, and 4.42MPa at 4000m respectively while the cohesive strength and elastic modulus increased from 6.89MPa, and 7,003.8MPa at 3500m to 7.52MPa, and 12,312.9MPa respectively at 4000m (Tables 1 and 2 and Figure 2c). A decrease in bulk and grain compressibilities and shear modulus is consistent with increasing depth in all the wells across the field. Poisson's ratio was influenced by rock mineralogy and the effect of depth was not significant on its value. Generally all shales irrespective of depth has a Poisson ratio ranging from 0.33 – 0.40, the value increasing with decreasing sand volume. Poisson ratio also increased with increase in elastic modulus in shale and decrease with increase in elastic modulus (Figures 3a and b).

The effect of porosity was also strong on the mechanical property evolution as high porosity rocks had lower strength in both shales and sandstones (Figures 4a and b). Rock strength has an indirect relationship with the shear modulus decreasing in both sandstones and shales (Figures 5a and b) and also with the volume of shale further asserting that shales are weaker rocks than sandstones (Figures 6 and 7). Elastic modulus increases with increasing vertical stress and by implication the depth of burial (Figures 8a and b). Rock matrix, bulk modulus, modulus and rock strength also increases with increase in vertical stress (Figures 9, 10 and 11) respectively while the rock compressibility decreases under

Table 2: Typical Rock Strength and Petrophysical Properties

Well	Depth(m)	Rock Strength Parameters						Petrophysical Parameters	
Well 10		Rock Type	UCSMPa	C_oMPa	T_oMPa	τ_iMPa	FA(V_p)(deg)	V_{sh}(frac)	Φ_{eff}(frac)
	2000	Shale	24.95	6.45	2.08	8.60	14.5	0.60	0.22
	2500	Shale	20.68	6.51	1.72	1.99E+15	15.5	0.27	0.10
	3000	Shale	23.99	6.78	1.99	1.43E+15	14.8	0.54	0.20
	3500	Sandstone	89.03	6.89	7.42	1.05E+15	0	0.43	0.07
Well 11	4000	Sandstone	53.06	7.52	4.42	3.99E+14	7.4	0.42	0.0008
	1500	Shale	20.21	5.8	1.68	7.17E-14	16	0.19	0.26
	2000	Shale	24.78	6.14	2.06	1.95E-13	17	0.59	0.23
	2500	Shaly SST	32.11	6.59	2.69	4.51E-13	13	0.05	0.10
	3000	Shaly SST	38.79	7.14	2.89	1.78E-13	7	0.33	0.12
	3500	Sandstone	78.44	7.35	6.64	3.4E-13	4	0.64	0.09
Well 05	4000	Sandstone	57.33	7.45	4.78	5.19E-13	2	0.59	0.17
	2000	Shale	15.39	9.99	1.28	5.52E-5	87	0.02	0.25
	2500	Shale	28.84	10.34	2.40	5.0E-7	87	0.11	0.33
	3000	Sandstone	52.32	10.34	4.36	4.27E-7	88	0.17	0.09
	3500	Sandstone	67.22	9.99	5.60	4.5E-7	88	0.05	0.21
	4000	Sandstone	57.13	9.99	4.76	4.93E-7	88	0.24	0.11

Note: SST = sandstone, UCS = unconfined compressive strength, C_o = cohesive strength, T_o = tensile strength, ϕ_i = initial shear strength, $FA_{(NPHI)}$ = angle of friction from neutron – porosity log, $FA_{(Vp)}$ = angle of friction from p-wave velocity, V_{sh} = volume of shale, Φ_{eff} = effective porosity.

the weight of the overlying rocks. Increasing depth, bulk density and vertical stress due to overburden loading led to higher degree of compaction resulting to higher mechanical strength as revealed by uniaxial compressive strength, cohesive strength and tensile strength in both shale and sandstones. Shales are more elastic and consequently are not prone to accidental fracturing relative to sandstones which fail under tension at lower pressures of the mud weight during drilling. In hydraulic fracturing operations, sandstones will propagate fractures at a lower injection pressure than shale. On the other hand, shales are more prone to shear failure than sandstones due to their low strength and high elasticity. The shale cap rocks are ductile, stiffer, less compressible and more prone to compressive shear failure. Mechanical heterogeneity across the field was caused by porosity, pore pressure, compartmentalization and depositional sequence.

Increase in effective overburden stress due to gravity loading and fluids expulsion causes grain sliding in shear and compaction deformation with reduction in the bulk and grain compressibilities as well as the pore volume of the sediment with

Figure 3a: Typical Young's Modulus Vs. Poisson Ratio Relationship in Shale

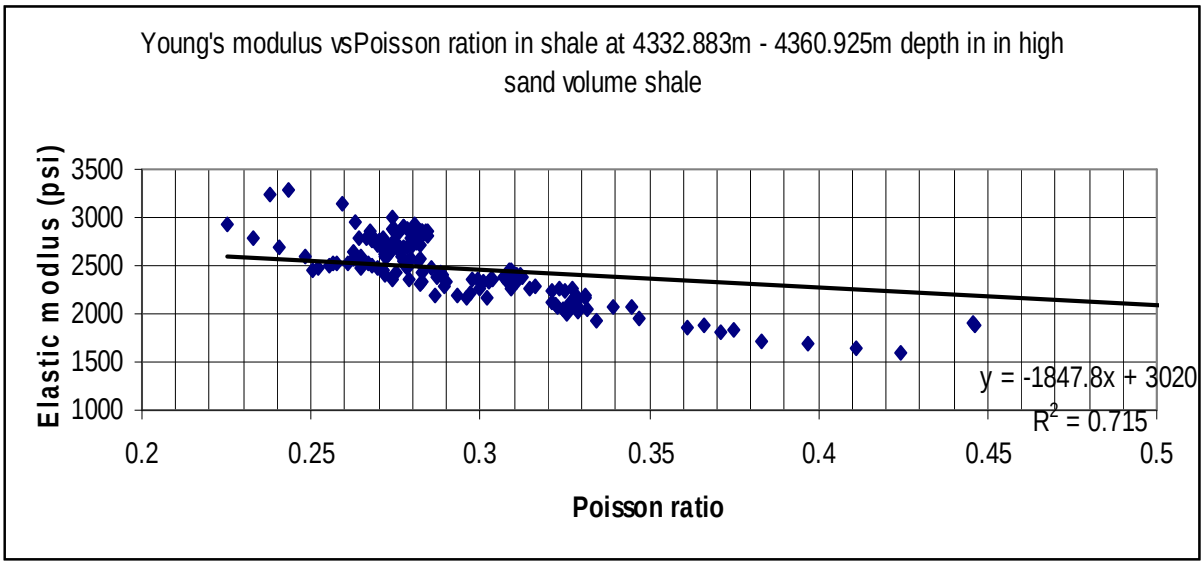

Figure 3b: Typical Young's Modulus Vs. Poisson Ratio Relationship in Reservoir Sandstone

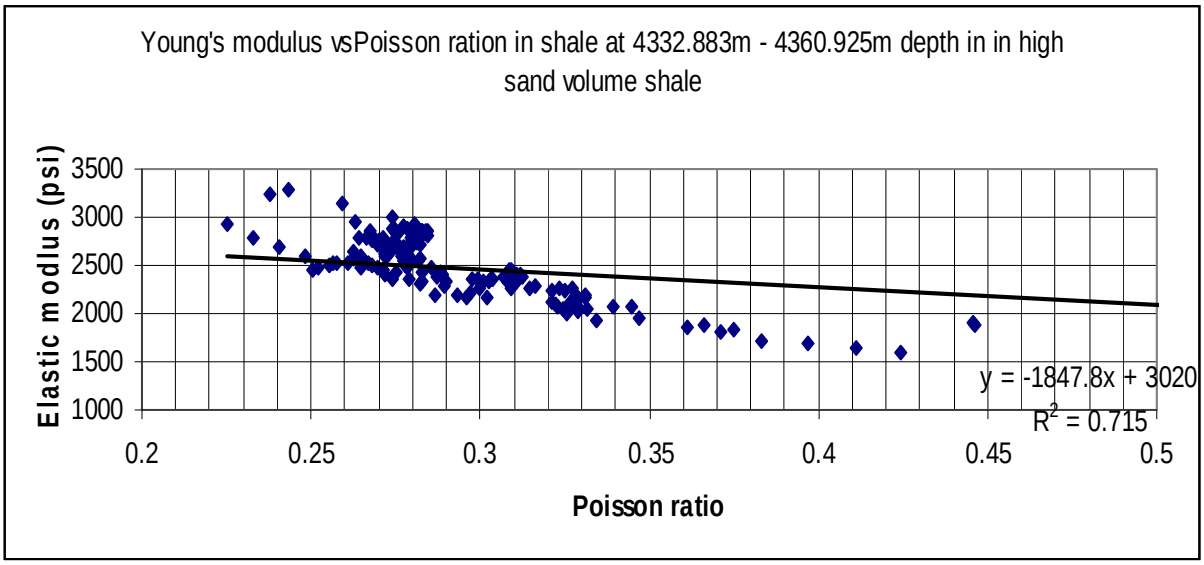

depth. Compaction lead to reduction in porosity and porosity changes even at very small strains affects the absolute permeability, wettability and capillary pressure.

Grain to grain contact destroys the cement bonds and closes the packing of individual grains by elastic distortions and strains. Since the impermeable and saturated with an

Figure 4a: Typical Porosity - Uniaxial Compressive Strength Bivariate Relationship in Shale

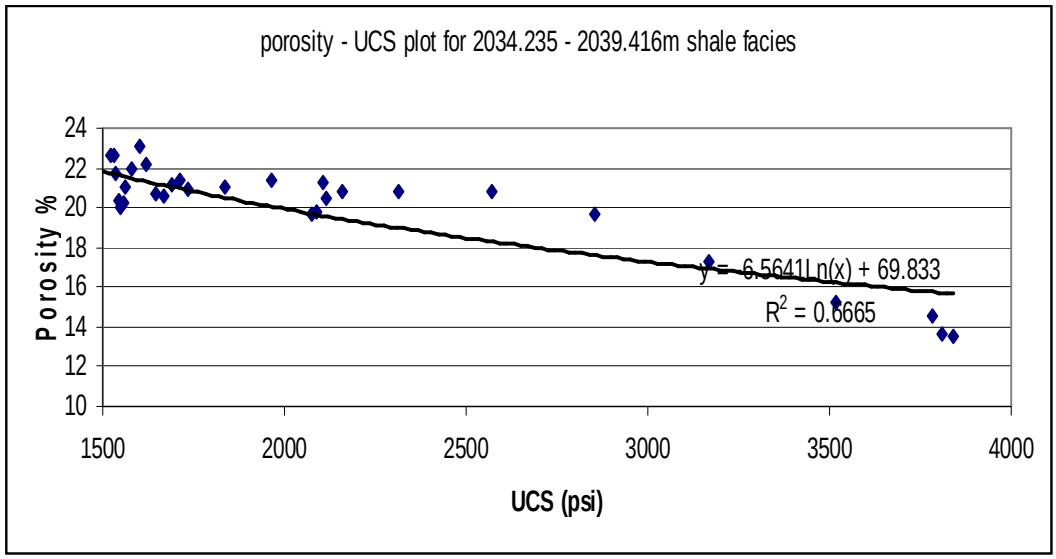

Figure 4b: Typical Porosity - Uniaxial Compressive Strength Bivariate Relationship in Sandstone

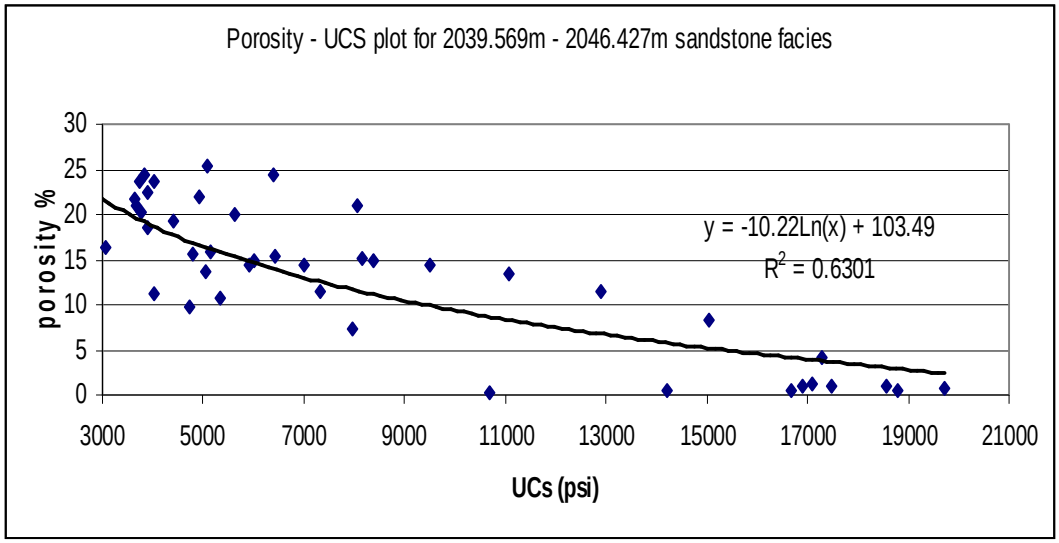

incompressible fluid, elastic deformation ensues and when there is disequilibrium compaction, abnormal pore pressures are generated as reported in most fields in the Niger Delta (Opara 2011, O'Conor et al 2011). Young tertiary sedimentary rocks deform primarily by compaction resulting in progressive loss of porosity with increasing depth of burial (Barnejee

and Muhiri 2013).The mechanisms of over-pressures generation in the shale is believed to be due to compressional inversion, tensile failure linked to gas generation at peak burial, shale diapirism and compaction disequilibrium where rapid burial leads to partial dewatering during diagenesis.

Figure 5a: Typical Variation of Uniaxial Compressive Strength With Shear Modulus in Shale

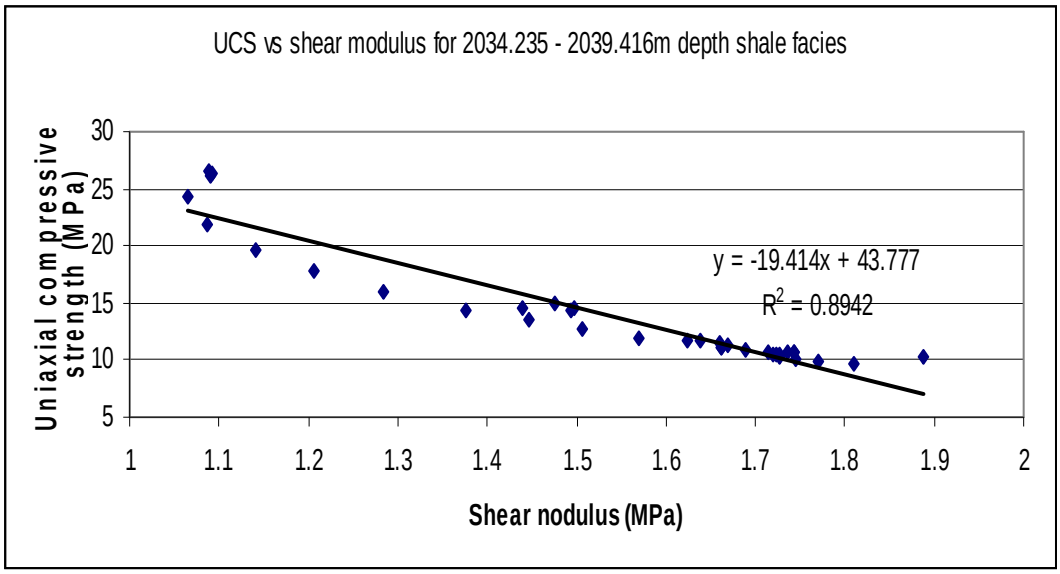

Figure 5b: Typical Variation Of Uniaxial Compressive Strength With Shear Modulus in Sandstone

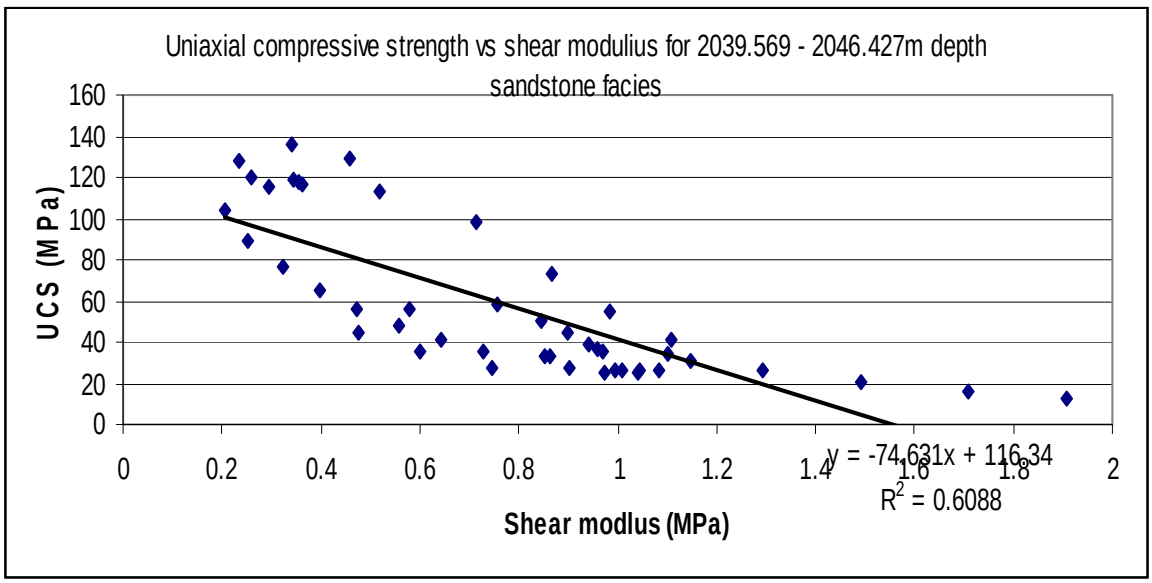

Figure 8a: Typical Variation Of Vertical Stress With Young's Modulus In Shale

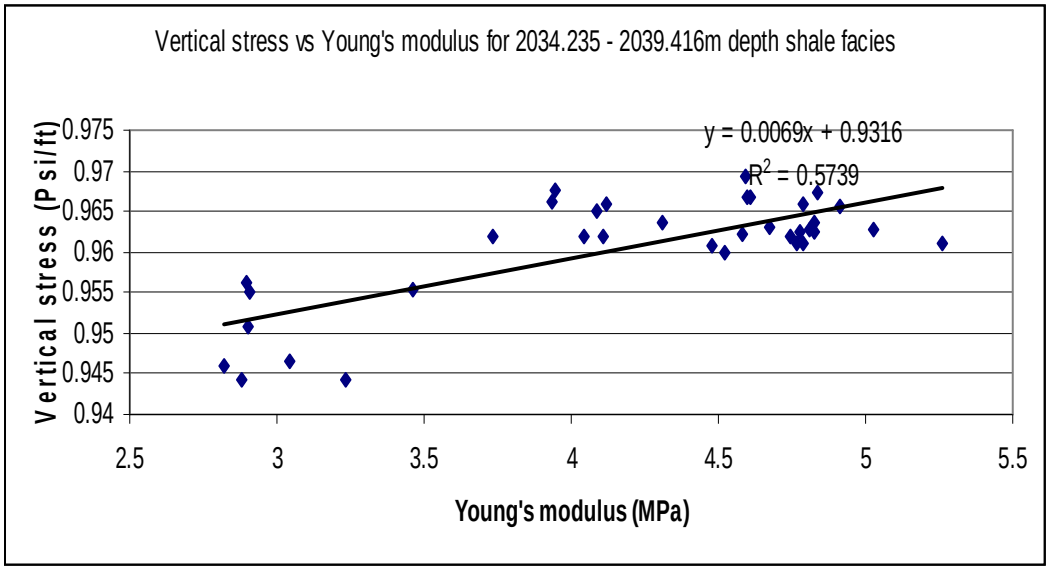

Figure 8b: Typical Variation Of Vertical Stress With Young's Modulus In Sandstone

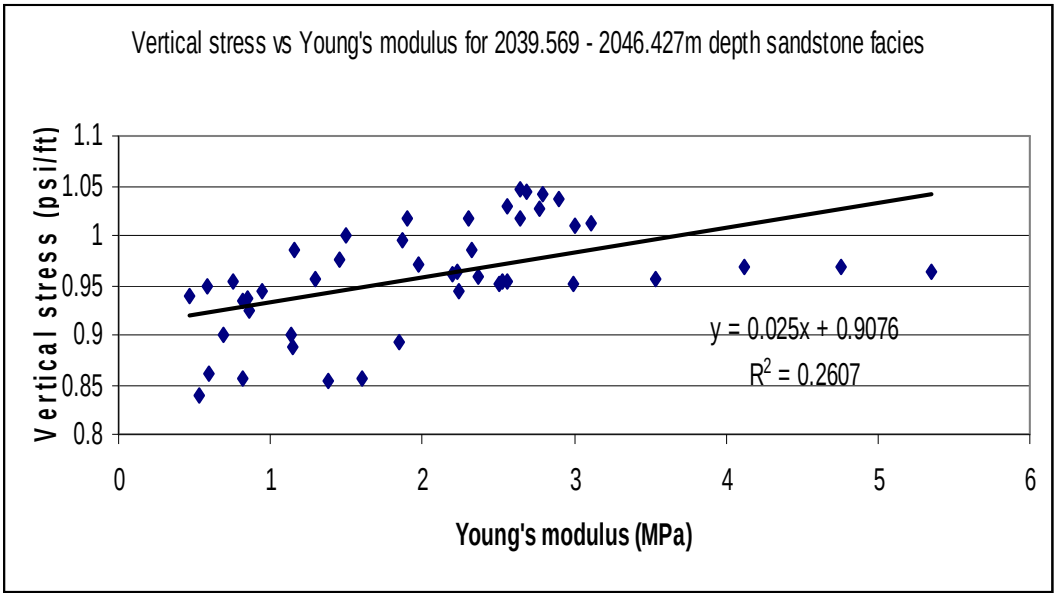

Correlation of the properties across the field (Figure 12) shows higher values of elastic, bulk and rigidity moduli in the east direction and a lateral decrease in the magnitude of the rigidity modulus from well 10 on the east to well 11 on the west depicting decrease in present day deformation.

Mechanics of Growth Faulting and Hydrocarbon Trapping

Rocks are very sensitive in their mechanical response to stress and stress causes them to have different strengths under tension and compression. They fracture through crack propagation when small strains are applied on them consequently most rocks are brittle. A

Figure 9a: Typical Variation Of Vertical Stress With Rock Matrix Modulus In Sandstone

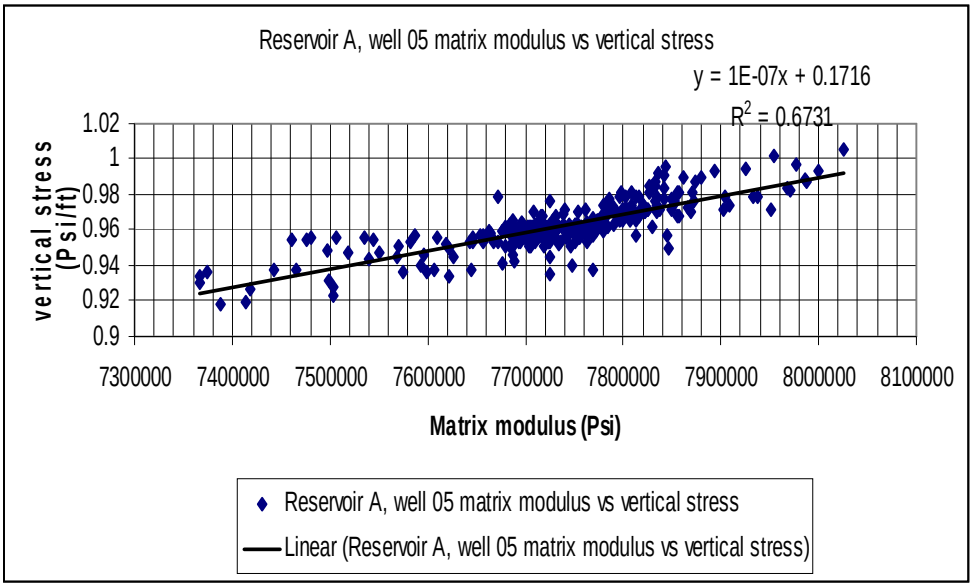

Figure 10: Typical Variation Of Vertical Stress With Tensile Strength In Sandstone

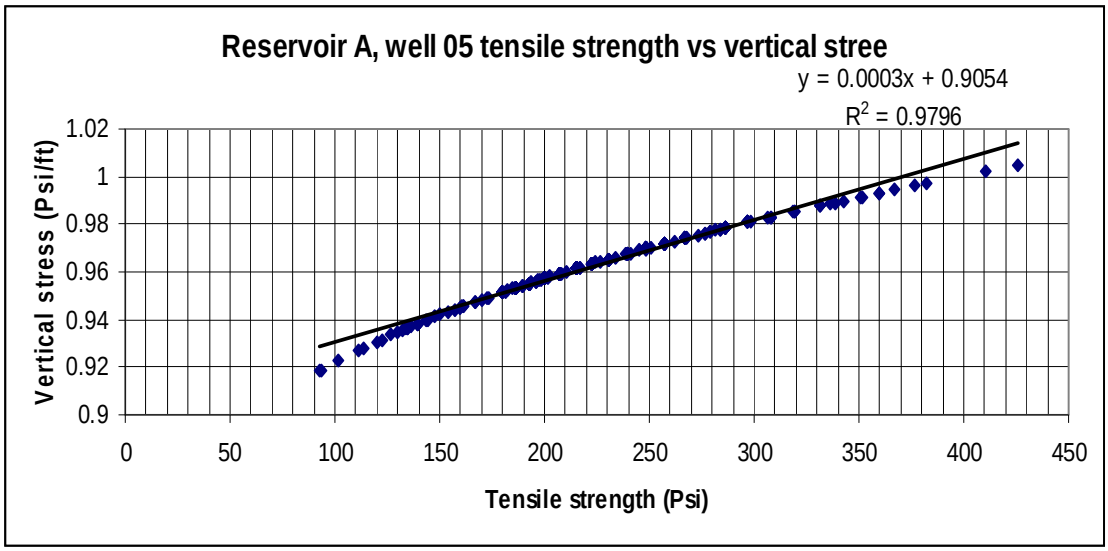

Figure 11: Typical Variation Vertical Stress With Rock Grain Compressibility in Sandstone Stone

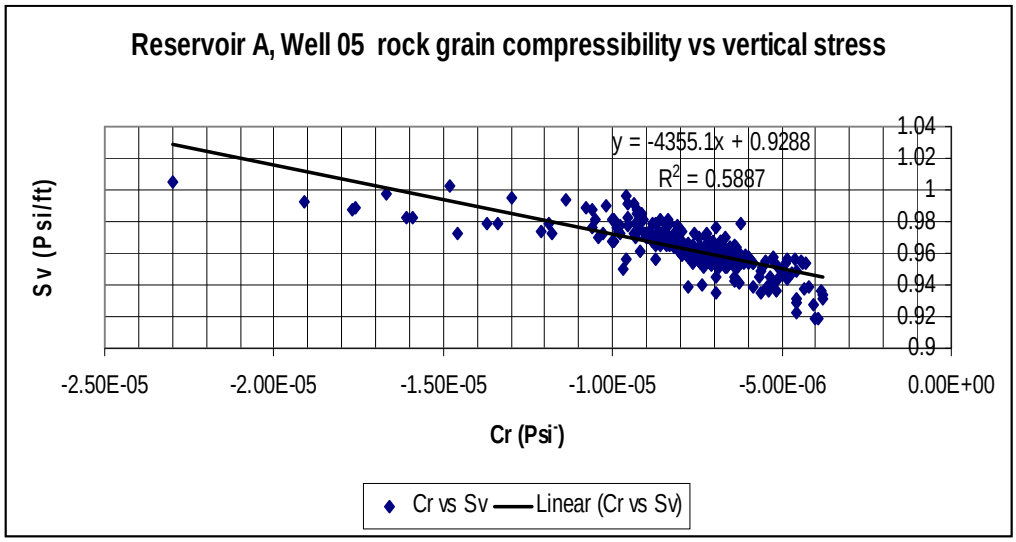

Figure 12: 1D Geomechanical Model and Facies Correlation in the Field

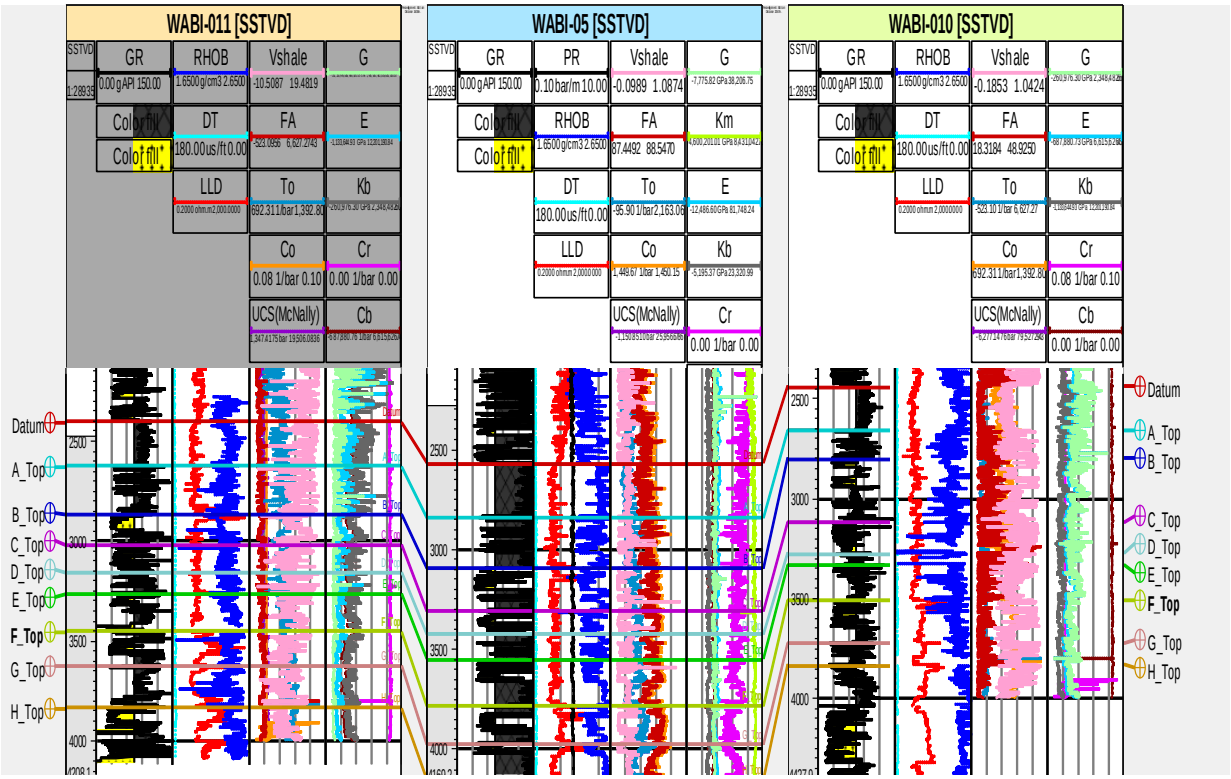

Figure 13: Depth Structure Map of the Field

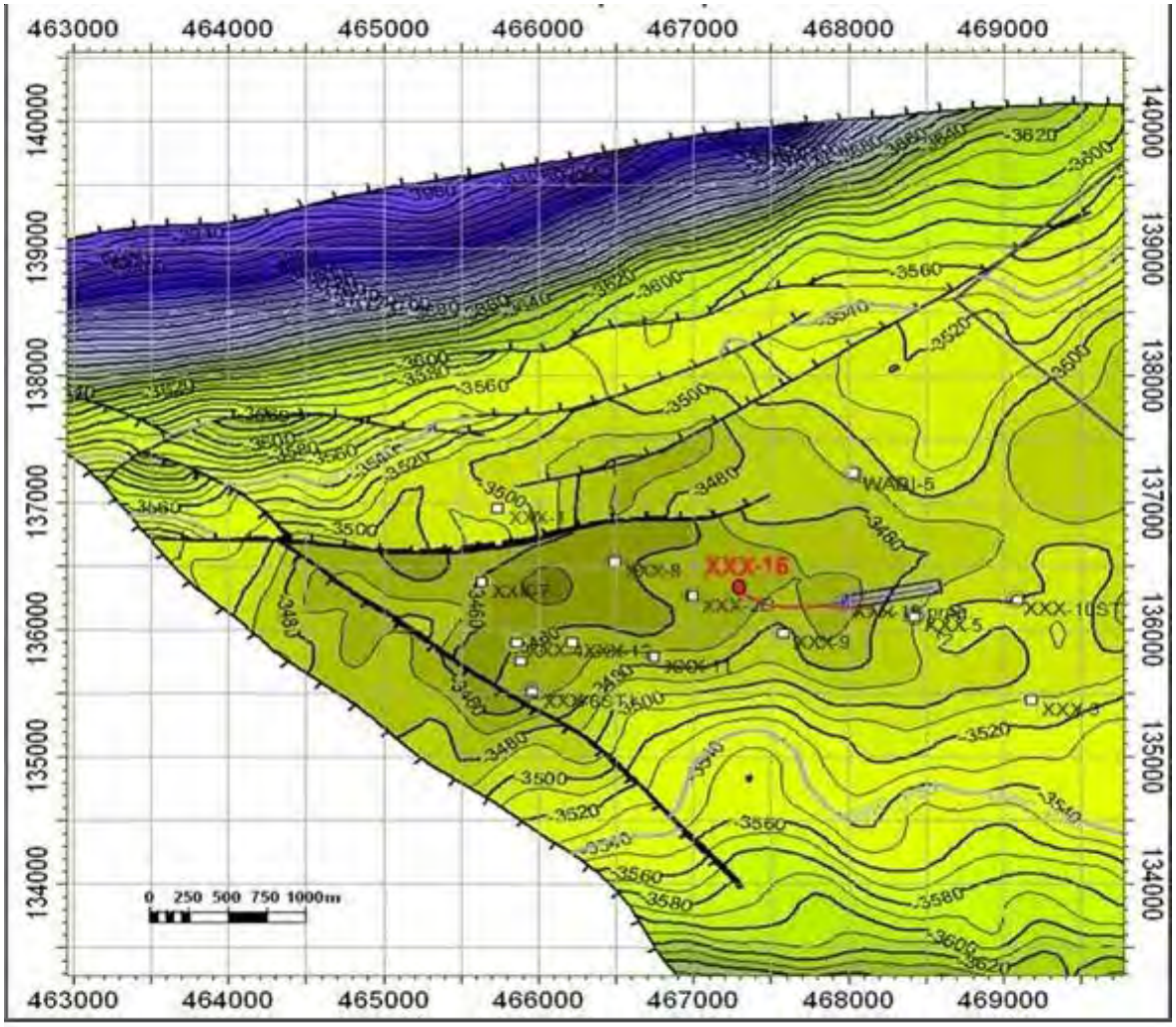

Source: Total E&P Ltd.

characteristic strain softening behavior occurs in which gradual decrease in strength with deformation leads to reduction in volume, distortion of shape and dilation at dense initial parking that follows the law of plasticity (Runesson 2006). In the field of study, tectonic induced tensile fracturing and faulting in response to directed stress at magnitudes higher than the yield strength of the rocks, on the flanks of the field created NE – SW and NW – SE trending listric faults followed by synkinematic downwarping of the downwthrown block and forming a grabben. This processes and actions created a depositional centre that was accompanied by rapid sedimentation of offlaping cycles of siliciclastic materials as reported in the basin wide delta scenario (Stacher 1995), depositing intervening sequences of marine

shales and sands. Increasing depth of burial and effective vertical stress accompanied by low rate of fluids diffusion, imposition of most of the overburden load on; and being borne by the pore fluids caused shear enhanced compaction accompanied by vertical fluid transfer along the faults and centroid effects in which initially flat sandstone beds surrounded by overpressured shales were loaded asymmetrically and tilted, creating a hydrostatic pressure in the sandstone and migration of hydrocarbons into the porous reservoir. Shales are impermeable and when saturated with incompressible fluids, elastic deformation is prevented thus generating excess pore pressures which top vary across the field from 1976m to 2248m, with the depocentre having a shallower depth. Increasing deposition and burial depth enhanced grain sliding in shear; reduction in the rock compressibility and pore volume, destruction of cement bonding in the reservoirs sands. At the same time, post depositional diagenetic reactions within the overpressured shales favoured undercompaction creating a disequilibrium that was facilitated by tectonic compaction induced by syndepositional re-orientation of the tectonic stresses during the Oligocene to Early Miocene. Continuous and rapid progradation in the depocentre further increased the bed thickness, effective vertical stress together with the tectonic stress re-orientation; anisotropy induced greater stress variations and differential mechanical response between the shales and the sand units. The imposed vertical stress and re-orientation of the horizontal stresses resulted in increased shale elasticity and destruction in cement bonding due to tensile microfracturing and closer packing of the sand units. This process caused a change in the azimuth of the NE-SW and NW-SE normal faults at greater depth due to elastic deformation under shear, forcing the faults to dilate and spread out laterally under gravity and developing into growth faults at depths of 3520 – 3600m. Line and shape structural restoration of the field and measurements depicted the growth index of these faults to average 1.99 and 1.11 on east and west respectively (table 1, figs. 12 and 13). Shale diapirism due to loading of poorly compacted shales from the lower Akata Formation, the continental intercalaire is also a causal factor that favours growth faulting and these faults continue to grow until they are constrained by adjacent formations.

The accompanying changes in rock volume and structural style depend on the rock mechanical properties of the specific lithologic unit, its porosity, cementation and burial depth.

Enhanced rapid deposition after the gravity faulting, syndepositional compressive and shear stresses acting within the formation causes a rotational movement of the beds and leading to the formation of rollover structures on the arm and tilting towards the growth faults. The sequences of the sand beds on these rollover anticlinal structures forms the reservoirs while the shale beds form the cap rocks and smears on the faults providing containment of the hydrocarbon within the sands. Doust and Omatsola (1990) observed that gravity faulting mostly offset different parts of the Agbada Formation and flatten into detachment planes near the top of the Akata Formation and this faulting style is reportedly prevalent in the basin (Weber and Daokoru 1977) as seen in the field of study, causing the downthrown block to remain an active sedimentation centre after their formation.

Conclusion

The geomechanical responses during the basin evolution has created porous and permeable sandstone reservoirs and stratigraphic as well structural traps during the synsedimentary compaction and tectonic deformation of the Agbada paralic sequence in response to increasing instability of the under-compacted, over-pressured shales and hydrocarbon migration into the sandstone tertiary petroleum system. The depositional environment so created offers conditions favourable for hydrocarbons migration from the basal Akata Formation, the major source rock of the basin through the fault conduits into the reservoir sand units while the shale provide capping above and sealing of the fault limbs thus providing good trapping mechanism for containment.

Acknowledgment

The author would like to thank Total Exploration and production Nigeria Ltd and the Department of petroleum Resources, Port Harcourt, Nigeria for providing data for this research.

References

1. Abija F A and Tse A C (2016), "In Situ Stress Magnitude and Orientation in an Onshore Field, Eastern Niger Delta: Implications for Directional Drilling", SPE 184234-MS, pp. 1 -15.
2. Anderson T L (2006), *Fracture Mechanics: Fundamentals and Applications*, 3rd Edition, Boca Raton, CRC Press, Florida.
3. Azizi V and Memarian H (2006), "Estimation of Geomechanical Parameters of Reservoir Rocks, Using Conventional Porosity Log", 4th Asian Rock Mechanics Symposium, Rock Mechanics in Underground Construction.
4. Banerjee S and Muhuri S (2013), "Applications of Geomechanics: Based Restoration in Structural Analysis Along Passive Margin Settings, Deep Water Niger Delta Example", in New Understanding of the Petroleum System of Continental Margins of the World.
5. Biot M A (1941), "General Theory of Three Dimensional Consolidation", *J. Appl. Phys.*, Vol. 12, No. 2, pp. 155-164. http://dx.doi.org/10.1063/1.1712886.
6. Bruno M S (2001), "Geomechanical Analysis and Decision Analysis for Mitigating Compaction Related Casing Damage", SPE 71695, pp. 1-13.
7. Chang C, Zoback M and Khalsar A (2006), "Empirical Relations Between Rock Strength and Physical Properties in Sedimentary Rocks", *Journal of Petroleum Science and Engineering*, Vol. 51, pp. 223-237.
8. Cleary J M (1958), "Hydraulic Fracture Theory: Part 1 – Mechanics of Materials", Illinois State Geological Survey Circular 251, pp. 1-25.
9. Coates G R and Denoo S A (1981), "Mechanical Properties Programme Using Borehole Analysis and Mohr Circle", SPWLA, 22nd Annual Logging Symposium.
10. Cook J, Rene A F, Hasbo K, Green S, Judzis A, Martiu J W, Suarez-Rivera R, Jorg H, Hooyman P, Lee D, Noerth S, Sayers C, Koutsabelloulis N, Marsden R, Stage M G and Tan C P (2007), "Rocks Matter: Ground Truth in Geomechanics", *Oil Review*, pp. 36-55.

11. Crain E R and Holgate D (2004), "Digital Log to Mechanical Rock Properties for Stimulation Design", *Focus*, pp. 1-9, Geoconvention.

12. Doust H and Omatsola E (1990), "Niger Delta", in J D Edwards and P A Santogrossi (Eds.), *Divergent/passive Margin Basins*, pp. 239-248, AAPG Memoir 48, Tulsa, AAPG.

13. Evamy B D, Haremboure J, Kamerling P, Knaap W A, Molloy F A and Rowlands P H (1978), "Hydrocarbon Habitat of Tertiary Niger Delta", *AAPG Bull.*, Vol. 62, pp. 277-298.

14. Fjaer E, Holt R M, Horsrud P, Raaen A M and Risnes R (2008), *Petroleum Related Rock Mechanics*, Amsterdam, Elsevier.

15. Geerstma J (1973), "Land Subsidence Above Compacting Oil and Gas Reservoirs", *J. of Petroleum Technology*, Vol. 25, pp. 734-744.

16. Greenberg M L and Castagna J P (1993), "Shear Wave Velocity Estimation in Porous Rocks", *Theoretical formulations: Preliminary Verification and Application. Geophysical Prospecting*, Vol. 40, pp. 195-209.

17. Hospers J (1965), "Gravity Field and Structure of the Niger Delta, Nigeria, West Africa", *Geological Society of American Bulletin*, Vol. 76, pp. 407-422.

18. Hudson J A and Harrison J P (1997), *Engineering Rock Mechanics; An Introduction to the Principles,* Elservier Science Ltd., p. 444, Oxford.

19. Jones M E, Leddra M J, Goldsmith A S and Edwards D (1992), "The Geomechanical Characteristics of Reservoirs and Reservoir Rocks", HSE - Offshore Technology Report, OTH 90, 333, pp. 1-202.

20. Kaplan A, Lusser C U and Norton I O (1994), "Tectonic Map of the World, Panel 10", Tulsa, American Association of Petroleum Geologists, Scale 1:10,000,000.

21. Kulke H (1995), "Nigeria", in H Kulke (Ed.) "*Regional Petroleum Geology of the World. Part II: Africa, America, Australia and Antarctica,* pp. 143-172, Gebrüder Borntraeger, Berlin.

22. Lal M (1999), "Shale Stability: Drilling Fluid Interaction and Shale Strength", SPE Asia Pacific Oil and Gas Conference and Exhibition, SPE 54356, pp. 20-22.

23. Larinov V (1962), *Borehole Radiometry*, USSR Nedra, Moscow.

24. Lehner P and De Ruiter P A C (1977), "Structural History of Atlantic Margin of Africa", *American Association of Petroleum Geologists Bulletin*, Vol. 61, pp. 961-981.

25. McNally G H (1987), "Estimation of Coal Measures Rock Strength Using Sonic and Neutron Logs", *Geoexploration*, Vol. 24, pp. 381-395.

26. Moos D (2006), "Geomechanics Applied to Drilling Engineering", in W L Lake, and R F Mitchel (Eds.), *Drilling Engineering*, Vol. II, p. 173.

27. O'Connor S, Swarbrick R, Pindar B, Lucas O, Adesanya F, Adedayo A, Nwankwoagu K, Edwards A, Heller J and Kelly P (2011), "Pore Pressure Prediction in the Niger Delta – Lessons Learnt From Regional Analysis", NAPE, Lagos Conference Paper Extended Abstract.

28. Opara A I (2011), "Estimation of Multiple Sources of Overpressures Using Vertical Effective Stress Approach: A Case Study of Niger Delta", *Petroleum and Coal*, Vol. 53, No. 4, pp. 302-314.

29. Paul P and Zoback M (2008), "Wellbore Stability Study for the SAFOD Borehole Through the San Andreas Fault", SPE 102781, pp. 394-408.

30. Pietro T, Giuseppe G, Massimiliano F, Anthony S and Dale W (2010), "Land Uplift Due to Subsurface Injection", *Journal of Geodynamics,* Vol. 51, No. 1, pp. 1-17.

31. Runesson K (2006), "Constitutive Modeling of Engineering Materials – Theory and Computation, the Primer", Lecture Notes, Department of Applied Mechanics, Calmers University of Technology, Goteborg.

32. Schlumberger (1989), *Log Interpretation: Principles/Applications,* pp. 1-1 – 13-19, Schlumberger Educational Services, Houston.

33. Sinha B K, Wang J, Kisra S, Li J, Pistre V, Bratton T and Sanders M (2008), "Estimation of Formation Stresses Using Borehole Sonic Data", Society of Petrophysist and Well Log Analyst 49th Annual Logging Symposium, pp. 1-16.

34. Short K C and Stäuble A J (1965), "Outline of geology of Niger Delta", *American Association of Petroleum Geologists Bulletin*, Vol. 51, pp. 761-779.

35. Stacher P (1995), "Present Understanding of the Niger Delta Hydrocarbon Habitat, in M N Oti and G Postma (Eds.), *Geology of Deltas*, pp. 257-267, A.A. Balkema, Rotterdam.

36. Turner J P, Healy D, Hillis R R and Welch M J (2017), "Geomechanics and Geology: Introduction", in *Geomechanics and Geology*, Vol. 458, pp. 7-29, Geological Society of London Special Publication. DOI:10.1144/SP 458.15

37. Wolf C, Russell C and Luis N (2005), "Log Based Pore Volume Compressibility – A Deep Water GoM Case Study", SPE 95545. pp. 1-10.

38. Weber K J and Daukoru E M (1975), "Petroleum Geology Aspects of the Niger Delta", *Proceedings of the Ninth World Petroleum Congress*, Volume 2, pp. 210-221, Geology, Applied Science Publishers, Ltd., London.

39. Zoback M D, Barton C A, Budy M, Castillo D A, Finkbeinerr T, Grollimund B R, Moos D B, Peska P, Ward C D and Wiprut D J (2003), "Determination of Stress Orientation and Magnitude in Deep Wells", *International Journal of Rock Mechanics and Mining Sciences*. Vol. 40, pp. 1049-1076.